2014 5th IEEE RAS & EMBS International Conference on
Biomedical Robotics and Biomechatronics (BioRob)
August 12-15, 2014. São Paulo, Brazil

Use of Surface Electromyography for Human Amplification Using an Exoskeleton Driven by Artificial Pneumatic Muscles

Joao Luiz A. S. Ramos, and Marco A. Meggiolaro

Abstract— **Robotics for rehabilitation and human amplification is imminent to become part of our daily life. The juxtaposition of human control capability and machine mechanical power offers a promising solution for human assistance and force enhancement. This paper presents an alternative and simple exoskeleton Human-Machine Interface (HMI) for human strength and endurance amplification using a modified version of the Hill-type muscle. Pneumatic Artificial Muscles (PAM) are used as actuators for its high power-to-weight ratio. Genetic Algorithms (GA) approach locally optimizes the control model parameters for the assistive device using muscle surface electromyography (sEMG). The proposed methodology offers advantages such as: reducing the number of electrodes needed to monitor the muscles, decreases the real-time processing effort, which is necessary for embedded implementation and portability, and brings the HMI to a neural level.**

Keywords-Exoskeleton; Electromyography; Hill Muscle Model; Human Amplification; Genetic Algorithms, Pneumatic Muscles

I. INTRODUCTION

Man and machine integration combines human control complexity with mechanical power, thus becoming very promising for human amplification.

The greatest challenge of uniting these two entities relies on developing a Human-Machine Interface (HMI) that can control the amplification device with the same naturalness and smoothness of the user movements. Many approaches with different physical quantities can be used including electromyography (EMG), electroencephalography (EEG), haptics, voice recognition, visual feedback, or some combinations of these [1]. The difficulty of using this type of bio-signals as continuous control commands is the time delay, the nonlinear and the nonstationary characteristics – in particular the EMG and EEG - they provide [2-5], and long learning process. Past studies [6-14] developed models to extract the desired information from these biological control variables, including black-box methods, such as Artificial Neural Networks (ANN), and mathematical models such as the Hill-type Muscle Model used in this work.

This work was supported in part by the *Fundação de Amparo à Pesquisa do Estado do Rio de Janeiro* (FAPERJ) and *Coordenação de Aperfeiçoamento de Pessoal de Nível Superior* (CAPES).
Ramos, J. L. is a PhD Student at the Massachusetts Institute of Technology - MIT (jlramos@mit.edu)
Meggiolaro, M. A. is a Professor from the Pontifical Catholic University of Rio de Janeiro, Brazil (meggi@puc-rio.br)

The HMIs developed so far usually demand a direct force feedback from the user or rather a very precise dynamic model of the exoskeleton in order to decrease its disturbance over the users movements [13]. Muscle natural signals are beneficial for anticipating these movements due to the electromechanical delay (EMD) from neural activation to muscle contraction [7].

The present work proposes a different methodology for estimating the torque applied to the upper-body exoskeleton joints using the processed and filtered muscular surface electromyography (sEMG). Making an approximation to the torque exerted by the user scaled by a nonlinear gain factor in order to control the input to the wearable robot. The 11kg exoskeleton performs the task of lifting a payload, while smoothly actuated by pneumatic artificial muscles (PAM) - which have an excellent power-to-weight ratio. The validation methodology adopted by this study is done by comparing the neural activation level with and without the assistive device.

This paper is organized in seven sections. Section II concerns the mechanical design of the exoskeleton that was used as a testbed, including the PAM model. Section III explains the Hill muscle model used to process the bio-signals and to estimate the control torque. Section IV shows the parameter optimization methodology using Genetic Algorithms (GA) and their calibration for different sessions. Section V regards the control of the exoskeleton and the test procedure while section VI shows the experimental results. Finally, section VII discusses the conclusions of this work and suggests future possibilities.

II. MECHANICAL DESIGN OF THE EXOSKELETON

The goal of the exoskeleton is to reduce human effort when lifting a payload. The mechanical design reduces the degrees of freedom (DOF) in order to complete the task with the simplest structure possible. In addition, as the exoskeleton is directly connected to the user, it is necessary to guarantee anthropomorphism and smoothness. Human's upper limb joint is capable of reaching a wide range of movement; however, it can develop limited torque [13]. Our solution proposes the use of artificial fluidic muscles to drive the system, due to the fact that it has an extremely high power-to-weight ratio: 1-1.5kW/kg compared to 50-100W/kg of electric actuators and 100-200W/kg of pneumatic and hydraulic ones [15].

A. The Pneumatic Artificial Muscle (PAM)

The PAM is composed of a rubber bladder with an inner fiber cloth. When air is pressurized it contracts axially

and expands radially, acting like a simple action cylinder. It can also be modeled as a nonlinear spring with a pressure-controlled stiffness [15].

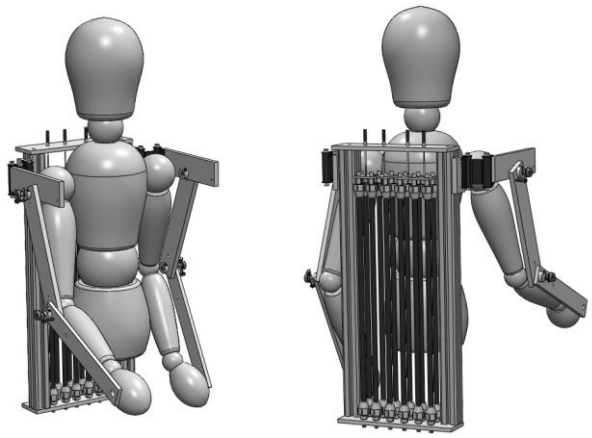

Fig. 1: Mechanical design of the exoskeleton.

The PAMs inherent compliance is useful for safety reasons; protecting the user from high jerk movements. But its nonlinearity is difficult to model and demands a complex controller. The force delivered is proportional to the inner pressure *P*, relative contraction *h* and contraction ratio *dh/dt* [16]. To determine the pressure needed to maintain a certain force *F* given a contraction is suggested in [15] by

$$F(P,h) = (aP + b)exp\left(\frac{1}{h+c}\right) + (dh + e)P + f. \quad (1)$$

The exponential function is the best candidate to model the high variation that can be evidenced by the PAM behavior. In (1), *a,b, c, d, e* and *f* are unknown parameters that need to be calibrated. The function *F(P,h)* is invertible and we obtain an analytical closed formula for the demanded pressure P_F given a certain contraction.

B. Degrees of Freedom (DOF)

The proposed design has three DOF, two of which are active. To lift a payload the shoulder and elbow flexion/extension are required; flexion actuation assistance is mandatory, while gravity is responsible for extension.

C. Determining the PAM

Human upper limb is capable of reaching a wide workspace. Although fluidic muscle can be very light and yet powerful, the main disadvantage is the low contraction capacity – approximately 20% of the nominal length at the maximum allowed pressure (8 bar for the MAS-10 [16]). Hence, the PAM required to achieve such range-to-load tradeoff is impractically long to be mounted directly over the arm link - which varies from 300-400mm.

To address that problem, we adopted a cable-driven transmission system which places the PAMs in a rear backpack enclosure, allowing these actuators to have a longer extension, such as [17] (see Fig. 1). The transmission system consists of a steel cable that slides inside steel tubes with an inner Teflon coat to reduce friction, the same as parking brake cables.

To increase the torque capacity, three PAMs were to actuate each joint. The entire exoskeleton is made of Aluminum 6061, weighting a total of 11kg (24,3lb).

III. The Hill Muscle Model

A. Muscle Force Estimation

The Hill-type muscle is a three-elements scheme (see Fig. 2) that models the muscle contraction-force relation. It was first developed by the Nobel Prize British physiologist Archibal Vivian Hill [18]. This straightforward method has a relatively high accuracy on predicting the muscle force using the EMG signal and its kinematic parameters. It defines a passive parallel element (PE), a passive series element (SE) and an active contractile element (CE).

The work in [7] and [19] proposes a model based on a set of equations for each muscle in order to predict the joint torque. However, the large set of muscles involved on the actuation of a single joint - about 12 for the elbow - presented by their work, demands a proportionally high number of equations and parameters, becoming costly for real-time applications. The present work modifies this method in two different ways: (i) it predicts the torque applied at the exoskeleton joint by the user instead of the torque at the user's articulation; and (ii) it uses only one representative muscle to estimate the torque activity generated by the muscle effort. The first one is sufficient to exclude any type of user sensoring – other than the sEMG's electrodes. The second one, on the other hand, reduces the computational effort for future embedded applications.

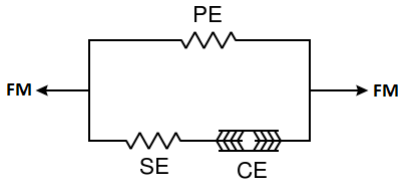

Fig. 2: The 3-element Hill-Type Muscle Model.

The neural activation is roughly defined as the intensity of the muscle sEMG. To model the signal nonlinearity and nonstationary behavior it is defined the relationship between the neural activation *a(t)* and the measured and amplified sEMG signal *u(t)* at time *t* as

$$a(t) = \frac{A^{u(t)}-1}{A-1}. \quad (2)$$

Parameter *A* defines the scale of nonlinearity between the two variables. The signal processing consists of:

- Analog signal amplification with instrumentation amplifier, gain of 805;
- Second-order Butterworth high-pass digital filter with 20Hz cut-off frequency;
- Digital full wave rectification;
- Second-order Butterworth low-pass digital filter with 2Hz cut-off frequency.

The first filter excludes the motion artifact due to skin impedance changes when it stretches and the third filter returns the envelope of the rectified signal.

From Fig. 2 we can extract three relations between the model parameters: (i) parallel elements share the same displacement (L); (ii) series elements share the same force (F); and (iii) the total force developed by the muscle is given by the sum of the forces on the parallel elements,

$$F_M = F_{CE} + F_{PE} = F_{SE} + F_{PE}. \quad (3)$$

According to this model, the force ($F_{PE,SE}$) exerted by the passive parallel and series elements is given by:

$$F_{PE,SE} = \frac{F_{max}}{(e^S - 1)}\left[e^{\frac{S\,\Delta L(t)}{\Delta L_{max}}} - 1\right], \quad (4)$$

where F_{max} is the maximal force made by each element, S is a shape parameter related to the muscle stiffness, and $\Delta L(t)$ and ΔL_{max} are the current and maximal contraction, respectively.

On the other hand, the active force made by the contractile element,

$$F_{CE} = a(t) f_l f_v F_{CEmax}, \quad (5)$$

is a function of the neural activation $a(t)$ and the normalized force-length f_l are given empirically by

$$f_l = exp\left(-0.5\left(\frac{\frac{\Delta L_{CE}(t)}{L_{CE0}} - \varphi_m}{\varphi_v}\right)^2\right). \quad (6)$$

It is modeled as a Gaussian function with mean value regulated using φ_m and φ_v, [7] and [19]. The normalized force-velocity f_v is taken as

$$f_v = \frac{0.1433}{0.1074 + exp\left(-1.3\,sinh\left(2.8\frac{V_{CE}(t)}{V_{CE0}(t)} + 1.64\right)\right)}. \quad (7)$$

In (5), F_{CEmax} is the maximal force that can be generated by the contractile element, and L_{CE0} is defined as the optimal fiber length, i.e., the position where the muscle can develop the maximum force. Furthermore, $\Delta L_{CE}(t)$ is the relative contraction, and $V_{CE}(t)$ the instantaneous contraction velocity. Moreover, $V_{CE0}(t)$ can be derived as a function of the neural activation $a(t)$ and the maximal velocity V_{CEmax}:

$$V_{CE0}(t) = 0.5(a(t) + 1)V_{CEmax}, \quad (8)$$

where

$$V_{CEmax} = 2L_{CE0}(1 + 4\alpha). \quad (9)$$

Other useful relations are

$$F_{PEmax} = 0.05 F_{CEmax}, \quad (10)$$

$$\Delta L_{PEmax} = L_{max} - (L_{CE0} + L_{Ts}), \quad (11)$$

$$F_{SEmax} = 1.3 F_{CEmax}, \quad (12)$$

$$\Delta L_{SEmax} = 0.03 L_{Ts}. \quad (13)$$

Constants α, L_{max}, and L_{Ts} are the percentage of fast fiber in the muscle, the maximal muscle length and the slack length, respectively.

We have verified empirically that the muscle instantaneous length could be obtained using the joint angular position (θ) in a third-order polynomial function

$$L_{CE}(\theta(t)) = a_3\theta(t)^3 + a_2\theta(t)^2 + a_1\theta(t) + a_0, \quad (14)$$

from which the muscle velocity can be obtained deriving (14) in respect to time, [20] and [21].

B. Exoskeleton Joint Torque Prediction

The work developed in [8] and [9] states that the muscle moment arm $r(\theta(t))$ varies with the joint angular position and when this variation is taken into account the torque prediction becomes more accurate. Through an analysis of the moment arm graphs as a function of the joint angle in [22], we propose that the relationship between these two variables can be approximately modeled by a third-order polynomial function,

$$r(\theta(t)) = b_3\theta(t)^3 + b_2\theta(t)^2 + b_1\theta(t) + b_0. \quad (15)$$

This moment arm also varies with the forearm pronation/supination angle, but in the present work this angle is fixed because this DOF is not allowed by the exoskeleton.

From equation (15) and the force estimated through the Hill model in the previous section, the joint torque can be predicted using

$$T_{exo} = K(t)T_M = K(t)[F_M r(\theta)], \quad (16)$$

where T_M is the torque produced by the exoskeleton, F_M is the PAM force, $r(\theta)$ is the instantaneous moment arm and $K(t)$ is the instantaneous gain factor. The contribution of the present study to the former Hill-type method relies on the use of $K(t)$ as well as (14) and (15). This nonlinear time-varying gain presents three advantages: (i) it establishes a relationship between the user single muscle force estimation with the exoskeleton joint torque prediction; (ii) it simplifies the model recalibration for every session and user; (iii) the recalibration process can be done using the exoskeleton itself and only a few measurements are needed.

We propose this gain factor function by analyzing empirically the exponential relationship between the torque developed by the exoskeleton T_{exo} and the user counterpart

T_M. As a result, taking into account the neural activation variation we define

$$K(t) = a(t)^{k_3} exp\big(k_2 + k_1 a(t)\big) + k_0, \quad (17)$$

Where, k_0, k_1, k_2, and k_3 are constants to be optimized.

IV. Parameter Estimation

In total, each muscle model has 22 real valued parameters to be estimated: 18 for the muscle model plus the extra four parameters necessary to define the gain *K(t)*. The PAM model, on the other hand, contains six constant values to be calibrated.

GA is a heuristic search optimization method capable of finding local minimum of functions with many variables. It is inspired by the survival of the fittest principle to estimate the next guess for the optimization iteration. Each guess is defined as a chromosome and after each iteration they are combined (crossover) and modified (mutation) to find the next estimation. This process continues until one of the termination criteria is achieved and the evolution terminates.

A. Pneumatic Muscle Model Optimization

In this section, we present the estimation of six constants (*a* to *f*) using *MatLab Genetic Algorithms Toolbox*. The fitness function to be minimized is the Root Mean Square Error (RMSE) between PAM model estimation and the *N* experimental values obtained for the muscles at each point *i*,

$$fit = \sqrt{\frac{1}{N}\sum_{i=1}^{N}\left(F_{exp}(i) - F_{GA}(i)\right)^2}. \quad (18)$$

B. Hill Muscle Model Optimization

To find the 22 constants for the physiological muscle model, a similar strategy is proposed. The torque applied to the exoskeleton by the limb is to be estimated using the Hill muscle model. The dynamic equation of the exoskeleton arm is used to calculate the instantaneous torque, which is then compared with the GA estimation. This equation is defined by the matricial equation

$$H(q)\ddot{q} + C(q,\dot{q})\dot{q} + G(q) = \tau, \quad (19)$$

where *H* is the inertia matrix, *C* is the centrifugal and Coriolis effect matrix, *G* is the gravitational torque vector, *q* is the state vector, and τ is the torque vector applied to the joints.

For the GA optimization the muscle force is calculated as follows:

1. The raw sEMG is filtered and the neural activation level is calculated using (2);
2. The exoskeleton joint angles are and then differentiated to estimate the joint velocities;
3. From the joints angles and velocities it is possible to calculate L_{CE}, ΔL_{CE}, V_{CE}, and *r*;
4. Hence, we obtain f_l, f_v and F_{CE}, which is equal to F_{CE}.
5. From equation (4) it is possible to find the SE displacement, add that value to the CE displacement to get the PE displacement;
6. Again from equation (4) we can calculate the force on PE and add that value to F_{CE} to obtain the total muscle force.
7. From F_M we can calculate T_{exo} using (16).

In this application, the RMSE function did not present satisfactory results as fitness function, hence we define the fitness function

$$fit2 = \sum_{i=1}^{N}\left|1 - \frac{F_{GA}(i)}{F_{dyn}(i)}\right|. \quad (24)$$

C. Model Calibration

As previously stated, the value of the sEMG will vary depending on anatomical and physiological characteristics. Variations between different sessions are expected because of changeable skin conditions and electrode placements. For that reason, it would be impractical to evolve the GA for another 2500 generations for every session and user for each joint. The solution found was to recalibrate the muscle model only evolving the gain factor *K(t)* parameters for every session (Fig. 3).

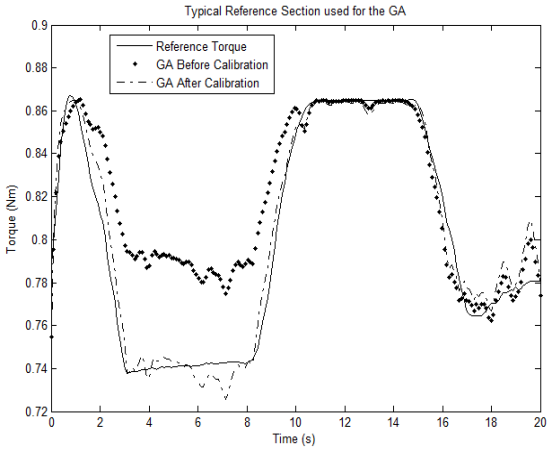

Fig. 3: Calibration session for GA.

V. Control of the Exoskeleton

The surface sEMG is recorded using GS27 pre-gelled disposable electrodes from *bio-medical* and the *Signa Gel* from *Parker Laboratories Inc*. Its amplification is done using the micro power instrumentation amplifier INA126P from *Texas Instruments*. The angles are obtained using two 10kΩ linear single turn potentiometers and the pressure is measured using the PX2 Series Heavy Duty Pressure Transducer from *Honeywell*. All the signals are acquired using the NI 9205 16 bits analog input card and the NI cDAQ 9172 chassis both from *National Instruments* at a 1.5kHz rate to avoid aliasing of the sEMG. To control the PAM the *Shadow Pneumatic Control Unit* (SPCU) was used [22]. The system is shown in Fig. 4.

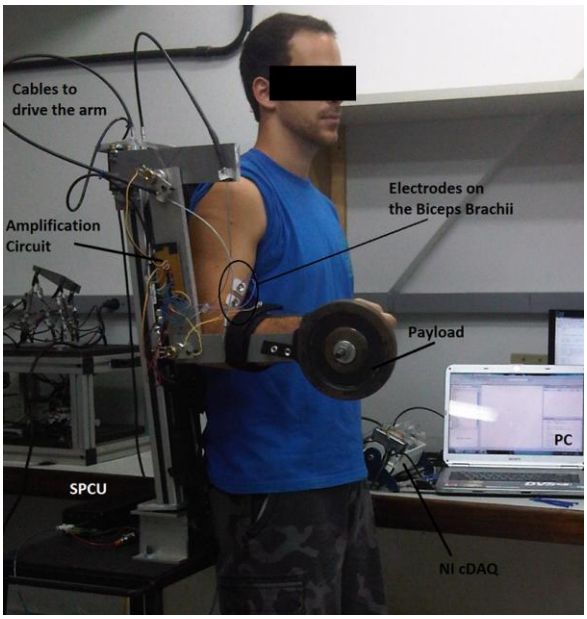

Fig. 4: The exoskeleton and the acquisition system.

The control loop works in the same way as the GA evaluate the chromosomes. Given the 22 parameters of the muscle model and the signal measured, it is possible to estimate the torque the user is applying on the exoskeleton joint. The controller then sends this information to the PAM model which drives the exoskeleton. On the other hand, the controller amplifies the torque by a given factor under the PAM limitations. As a result this proposed controller reduces the users effort to manipulate the payload. The control scheme can be viewed on Fig. 5. Given the pressure P_d necessary for the control, a proportional controller with gain *kp* was implemented to drive the system pressure P_{sys} to the desired reference.

VI. The Experimental Results

To validate the methodology presented, experimental tests are performed using the developed exoskeleton. The calibration process is fast and simple, taking about five minutes per joint. The calibration can be described by the following steps:

- The user is asked to move his or her arm and forearm together with the inactive exoskeleton through all the motion range and at different speeds: low, medium and high, depending on the user capabilities.
- The same process is repeated with a 3.1kg payload located at the end-effector of the exoskeleton.
- The software calibrates the muscle model running the GA for about 200 – 500 generations (which takes about two minutes).

Finally, the exoskeleton is ready to be used.

Fig. 6 shows the neural activation level when lifting a 3.1kg payload with the active and inactive exoskeleton and a torque amplification gain of 1.5. It is possible to verify a significant reduction on the effort done when lifting the load. The bottom graph shows the percentage of increase of the neural activation.

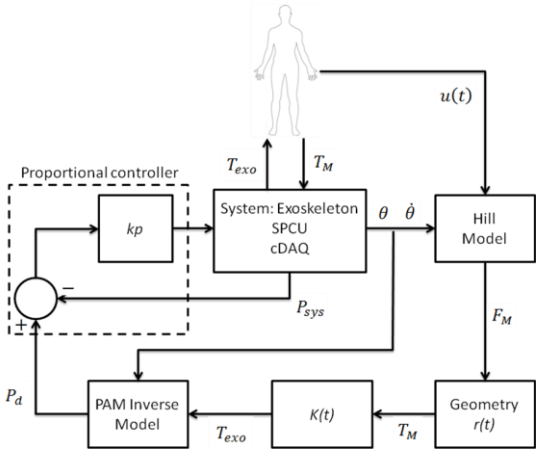

Fig. 5: Control architecture proposed.

Within static submaximal contractions both amplitude and frequency based analysis parameters show time domain changes due to muscular fatigue. The amplitude shows an increase whereas the frequency based mean or median of the total power spectrum shows a decrease over contraction time [4].

The second evaluation test concerns the endurance to muscular fatigue while wearing the assistive device. The shoulder joint sEMG is evaluated while under static load with the 3.1kg payload at an angle of approximately 35 degrees in respect to downward position during 1 minute (Fig. 7). The horizontal lines on the second plot represent the mean value of the sEMG at each condition.

It is possible to verify that while the exoskeleton is off the neural activation level is much higher (128% increase on the mean value). On this condition, the user cannot maintain the static angle and oscillations due to muscular fatigue start to occur, the sEMG signal amplitude also starts to grow. On the other hand, while the device is active, not only the neural activation level is considerably smaller, but the user is able to statically hold the payload.

VII. Conclusions

A sEMG-based controller was developed using a modified Hill-type muscle model to control an exoskeleton actuated by fluidic muscles. This type of actuator not only guarantees smoothness while being driven but can also generate large forces when compared to its own weight. It is then a good candidate for a lightweight wearable robot. An upper limb exoskeleton was designed from the chosen actuator.

For the control algorithm a Hill-type muscle model was used to estimate the torque applied directly over the exoskeleton joint. The proposed method introduces a nonlinear gain factor *K(t)* which is used to facilitate the recalibration of model parameters. The calibration process takes about five minutes for each joint and is able to converge in approximately 200-500 generations of the GA.

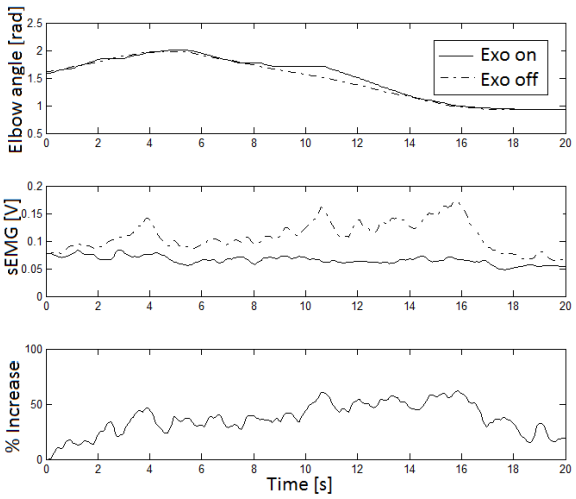

Fig. 6: Neural activation level with and without the exoskeleton assistance.

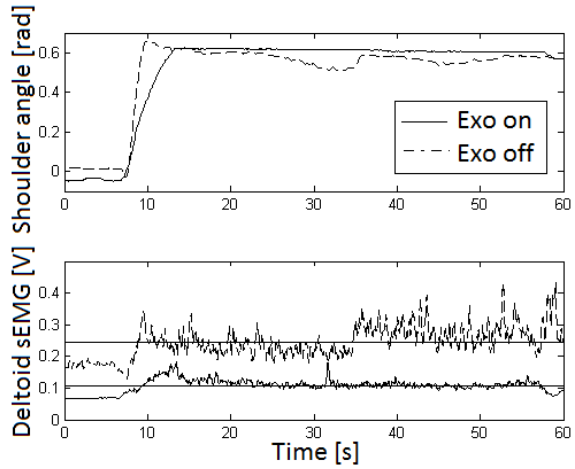

Fig. 7: Fatigue endurance with and without the exoskeleton assistance.

The task of lifting a payload was performed, showing that a torque gain factor of 1.5 is enough reduce the neural activation in about 67%. Also, maintaining static torque is facilitated, reducing de sEMG mean value in about 53%. The exoskeleton shares part of the torque necessary to lift the weight and the user supports only a reduced part of the load, increasing the user overall strength, avoiding fatigue and increasing endurance.

Future work embraces the development of an embedded controller to make the exoskeleton mobile and the optimization of the mechanical structure to reduce its weight.

REFERENCES

[1] Ormiga, A., "*Controle de um Manipulador Robótico Através de uma Interface Cérebro Máquina Não-Invasiva com Aprendizagem Mútua*", M.Sc. Dissertation, PUC-Rio, Rio de Janeiro, Brazil, August 2010.

[2] Rash, G.S., "*Electromyography Fundamentals*", DelSys Inc., 2003.

[3] De Luca, C. J. "*The Use of Surface Electromyography in Biomechanics*", Wartenweiler Memorial Lecture, The International Society for Biomechanics, 1993.

[4] Konrad, P., "*The ABC of EMG: Practical Introduction to Kinesiological Electromyography*", Version 1.0, 2005.

[5] "*Basics of Surface Electromyography Applied to Physical Rehabilitation and Biomechanics*", Thought Technology Ltd., 2009/2010

[6] Fleisher, C. "*Controlling Exoskeletons with EMG signals and a Biomechanical Body Model*", Ph.D. Thesis, Technical University of Berlin, Germany, 2007.

[7] Rose, J., Fuchs, M. B., Arcan, M., "*Performances of Hill-Type and Neural Network Muscle Models – Towards a Myosignal-Based Exoskeleton*", Department of Biomedical Engineering and Department of Solid Mechanics, Materials and Structures, Faculty of Engineering, Tel Aviv University, Israel, Setembro de 1998.

[8] Lloyd, D., Besier, T., "*An EMG-driven musculoskeletal model to estimate muscle forces and knee joint mometns in vivo*", Journal of Biomechanics, Elsevier, December 2002.

[9] Au, S., Bonato, P., Herr, H., "*An EMG-position controlled system for an active ankle-foot prosthesis: An initial experimental study*", 9th International Conference on Rehabilitation Robotics, Chicago, IL, USA, June 2005.

[10] Shao, Q., Bassett, N., Manal, K., Buchanan, T., "*An EMG-driven model to estimate muscles forces and joint moments in stroke patients*", Computers in Biology and Medicine, Elsevier, September 2009.

[11] Luh, J., Chang, G., Cheng, C., Lai, J., Kuo, e., "*Isoknetic elbow joint torques estimation from surface EMG and kinematic data: using an artificial neural network model*", Journal of Electromyography and Kinesiology, Elsevier, May 1998.

[12] Ullah, K., Khan, A., Islam, I., Khan, M., "*Electromyography (EMG) signal to joint torque processing and effect of various factors on EMG to torque model*", Journal of Engineering and Technology Research Vol. 3(12), November de 2011.

[13] Gopura, R. A. R. C., Kiguchi, K., "*Mechanical Designs of an Active Upper-Limb Exoskeleton Robots: State-of-the-Art and Design Difficulties*" 2009 IEEE, 11st International Conference on Rehabilitation Robotics, Kyoto International Conference Center, Japan, June 2009.

[14] Cavallaro, E., Rosen, J., Perry, J., Burns, S., "*Real-Time Myoprocessors for a Neural Controlled Powered Exoskeleton Arm*", IEEE Transactions on Biomedical Engineering, Vol. 53, No. 11, November 2006.

[15] Szepe, T., "*Accurate force function approximation for pneumatic artificial muscles*", Department of Technical Informatics, University of Szeged, Hungary.

[16] *Fluidic Muscle DMSP/MAS – Festo Catalogue*, FESTO, 2010.

[17] Kobayashi, H., Aida, T., and Hashimoto, T., "*Muscle Suit Development and Factory Application*", International Journal of Automation Technology Vol. 3, No. 6, 2009.

[18] Hill, A. V., "*The heat of shortening and the dynamic constants of muscle*", Proc. R. Soc. London Ser B, 126, (1938), pp. 136-195.

[19] Cavallaro, E., Rosen, J., Perry, J., Burns, S., Hannaford, B., "*Hill-Based Model as a Myoprocessor for a Neural Controlled Powered Exoskeleton Arm – Parameters Optimization*", International Conference on Robotics and Automation, Barcelona, Spain, April 2005.

[20] Rassier, D., MacIntosh, B., Herzog, W., "*Length dependence of active force production in skeletal muscle*", Journal of Applied Physiology, American Physiology Society, July 2012.

[21] Gordon, M., Huxley, A., Julian, F., "*The Variation in Isometric Tension with Sarcomere Length in Vertebrate Muscle Fibres*", Department of Physiology, University College London, September 1965